4404 *Inorg. Chem.* **2001,** *40,* 4404−4408

Synthesis and Characterization of the First Examples of Perfluoroalkyl-Substituted Trialkyloxonium Salts, $[(CH_3)_2OCF_3]^+[Sb_2F_{11}]^-$ and $[(CH_3)_2OCF(CF_3)_2]^+[Sb_2F_{11}]^-$

Rolf Minkwitz,* Stefan Reinemann, Raphael Seelbinder, and Detlef Konikowski

Anorganische Chemie, Fachbereich Chemie der Universität Dortmund, D-44221 Dortmund, Germany

Hans Hartl* and Irene Brüdgam

Institut für Anorganische und Analytische Chemie der Freien Universität Berlin,
D-14195 Berlin, Germany

Joachim Hegge, Berthold Hoge, Jeffrey A. Sheehy, and Karl O. Christe*

Loker Hydrocarbon Research Institute, University of Southern California, Los Angeles, California
90089, and Propulsion Sciences and Advanced Concepts Division, Air Force Research Laboratory,
Edwards Air Force Base, California 93524-7680

Received March 2, 2001

In the superacidic HF/SbF_5 system, methyl trifluoromethyl ether forms at −78 °C the new tertiary oxonium salt $[(CH_3)_2OCF_3]^+[Sb_2F_{11}]^-$, which was characterized by Raman and multinuclear NMR spectroscopy and its crystal structure. The same oxonium salt was also obtained by methylation of CH_3OCF_3 with CH_3F and SbF_5 in HF solution at −30 to −10 °C. Replacement of one methyl group in the trimethyloxonium cation by the bulkier and more electronegative trifluoromethyl group increases the remaining $O-CH_3$ bond lengths by 0.037(1) Å and the sum of the C−O−C bond angles by about 4.5°. Methylation of $CH_3OCF(CF_3)_2$ with CH_3F in HF/SbF_5 solution at −30 °C produces $[(CH_3)_2OCF(CF_3)_2]^+[Sb_2F_{11}]^-$. The observed structure and vibrational and NMR spectra were confirmed by theoretical studies at the B3LYP/6-311++G(2d,2p) and the MP2/6-311++G(2d,p) levels.

Introduction

Trialkyloxonium compounds were extensively investigated by Meerwein and are widely used as alkylating reagents.[1] Their reactivity can be further increased by using superacidic solutions.[2,3] Although the structures of trialkyloxonium ions are of great interest, only the crystal structures of $[(CH_3)_3O]^+[BF_4]^-$,[4] $[(Et)_3O]^+[BF_4]^-$, and $[(Ph)_3O]^+[B(Ph)_4]^-$ [5] are known. The structures of the OC_3 skeletons of these cations differ due to steric and electronic effects. Thus, C−O−C angles of 112−113° were observed for $[(CH_3)_3O]^+$, while for $[(Ph)_3O]^+$ a nearly planar arrangement with C−O−C angles of 120.1, 121.5, and 115.5° was found.

Since CF_3 groups require more space than methyl groups, a stepwise substitution of the methyl groups in $[(CH)_3O]^+$ by CF_3 groups should also lead to a more planar arrangement of the OC_3 skeleton. This principle was nicely demonstrated by Buerger and Oberhammer for the isoelectronic trimethylamines.[6] Using electron diffraction, they found that the C−N−C angle changes from a pyramidal 108.7° in trimethylamine[7−10] to a nearly planar 117.9° in $N(CF_3)_3$. It was therefore interesting to attempt the synthesis of the previously unknown[11] perfluoroalkyl-substituted tertiary oxonium ions and to study the influence of perfluoroalkyl substitution on the structure of these ions.

Experimental Section

All reactions were carried out using either Kel-F or Teflon-FEP reactors and stainless steel vacuum lines.[12] HF was dried either by treatment with fluorine or by storage over BiF_5.[13] Nonvolatile compounds were handled either in the dry N_2 atmosphere of a glovebox or by using standard Schlenk techniques. CH_3OCF_3 was prepared by a literature method.[14]

Raman spectra were recorded either on an ISA T64000 spectrometer using an Ar^+ laser (Spectra Physics, 514.5 nm) and a CCD detetctor (EEV CCD15-11) or on a Bruker Equinox 55 with an FRA 106/S Raman attachment using an Nd:YAG laser (Coherent, 939.4 nm). The NMR spectra in HF solution were recorded either at −65 °C with a Bruker DPX 300 spectrometer or at −30 to −10 °C with a Bruker

---

(1) Meerwein, H. *Methoden der Organische Chemie (Houben-Weyl)*, 3rd ed.; Thieme: Stuttgart, Germany, 1965; Vol. 6, p 325.
(2) Olah, G. A. *Angew. Chem., Int. Ed. Engl.* **1993**, *32*, 767.
(3) Hartz, N.; Rasul, G.; Olah, G. A. *J. Am. Chem. Soc.* **1993**, *115*, 1277.
(4) Minkwitz, R.; Meckstroth, W.; Hirsch, C.; Kornath, A. Unpublished results.
(5) Watkins, M. I.; Ip, W. M.; Olah, G. A.; Bau, R. *J. Am. Chem. Soc.* **1982**, *104*, 2365.
(6) Bürger, H.; Niepel, H.; Pawelke, G.; Oberhammer, H. *J. Mol. Struct.* **1979**, *54*, 159.
(7) Bodor, N.; Dewar, M. J.; Harget, A.; Haselbach, E. *J. Am. Chem. Soc.* **1970**, *92*, 3854.
(8) Hehre, W. J. *J. Am. Chem. Soc.* **1975**, *97*, 5308.
(9) Mastryukov, V. *S. J. Struct. Chem.* **1976**, *17*, 69.
(10) Charton, M. *J. Am. Chem. Soc.* **1979**, *101*, 7356.
(11) Olah, G. A.; Laali, K. K.; Wang, Q.; Surya Prakash, G. K. *Onium Ions;* Wiley: New York, 1998; Chapter 3.
(12) Christe, K. O.; Wilson, R. D.; Schack, C. J. *Inorg. Synth.* **1986**, *24*,3.
(13) Christe, K. O.; Wilson, W. W.; Schack, C. J. *J. Fluorine Chem.* **1978**, *11,* 71.
(14) Minkwitz, R.; Konikowski, D. *Z. Naturforsch.* **1996**, *51B*, 599.

10.1021/ic010239w CCC: $20.00

AM 360 using heat-sealed 3 mm i.d. Teflon-FEP tube liners (Wilmad Glass Co.). Single crystals were placed in Lindemann glass capillaries under a cold stream of dry nitrogen, and an X-ray diffraction study was carried out using a Nicolet R3m/V diffractometer.

Preparation of $[(CH_3)_2OCF_3]^+[Sb_2F_{11}]^-$. Method A. In a 50 mL Kel-F reactor, SbF_5 (2 mmol) was dissolved in 2 g of anhydrous HF. The solution was frozen at −196 °C, and CH_3OCF_3 (2 mmol) was condensed into the reactor. The mixture was warmed to −78 °C and kept at this temperature for 2 h. Volatile materials were removed under a dynamic vacuum at −78 °C. In the colorless solid residue, crystals suitable for X-ray diffraction studies were found.

In an 8 mm quartz tube, SbF_5 (1 mmol) was dissolved in 1 g of anhydrous HF. The solution was frozen at −196 °C, and CH_3OCF_3 (1 mmol) was condensed into the tube. The resulting solution was analyzed at −65 °C by ^{19}F NMR spectroscopy.

Method B. In a 65 mL Teflon-FEP reactor, containing a Teflon-coated magnetic stirring bar, SbF_5 (3.5 mmol) was dissolved in 5 mL of anhydrous HF, and CH_3F (10 mmol) was added at −196 °C. The mixture was homogenized at −78 °C, and CH_3OCF_3 (1.75 mmol) was added at −196 °C. The resulting mixture was stirred at −78 °C for 2 h, and then all volatile material was pumped off at this temperature. The remaining colorless solid (1.000 g, weight calcd for 1.75 mmol of $[(CH_3)_2OCF_3]^+[Sb_2F_{11}]^-$ 0.993 g) was identified by vibrational and multinuclear NMR spectroscopy as $[(CH_3)_2OCF_3]^+[Sb_2F_{11}]^-$.

Preparation of $[(CH_3)_2OCF(CF_3)_2]^+[Sb_2F_{11}]^-$. Following the procedure of Method B, described above for $[(CH_3)_2OCF_3]^+[Sb_2F_{11}]^-$, the title compound was prepared by methylation of $CH_3OCF(CF_3)_2$ and was characterized by multinuclear NMR spectroscopy.

Theoretical Calculations

Ab initio calculations were carried out for $[(CH_3)_2OCF_3]^+$, CH_3OCF_3, $[(CH_3)_3O]^+$, and CH_3OCH_3 using the B3LYP density functional method[15] and the 6-311++G(2d,2p)[16] basis set on IBM RS/6000 workstations. Optimized geometries and isotropic NMR shieldings were calculated using the GIAO-MBPT(2) approach,[17] which employs the gauge-including atomic orbital (GIAO) solution to the gauge-invariance problem.[18] Chemical shifts were obtained by referring these shieldings to those of the standard reference compounds tetramethylsilane and fluorotrichloromethane, which were computed at the same level of theory.

Results and Discussion

Formation and Stability of $[(CH_3)_2OCF_3]^+[Sb_2F_{11}]^-$. CH_3OCF_3 reacts with SbF_5 in HF solution at −78 °C to give $[(CH_3)_2OCF_3]^+[Sb_2F_{11}]^-$ as a crystalline and highly hydrolyzable solid in quantitative yield (eq 1). The use of AsF_5 as a Lewis acid does not give a stable product. The reaction mechanism for (1) was established[19] by multinuclear NMR spectroscopy. It involves the initial protonation of CH_3OCF_3 (eq 2). The resulting $[CH_3OHCF_3]^+$ cation then acts as a methylating agent to methylate a second CH_3OCF_3 molecule with formation of CF_3OH (eq 3), which is subsequently protonated to the $[CF_3OH_2]^+$ cation (eq 4).

$$2CH_3OCF_3 + 4SbF_5 + 2HF \rightarrow [(CH_3)_2OCF_3]^+[Sb_2F_{11}]^- + [CF_3OH_2]^+[Sb_2F_{11}]^- \quad (1)$$

$$CH_3OCF_3 + 2SbF_5 + HF \rightarrow [CH_3OHCF_3]^+[Sb_2F_{11}]^- \quad (2)$$

$$[CH_3OHCF_3]^+[Sb_2F_{11}]^- + CH_3OCF_3 \rightarrow [(CH_3)_2OCF_3]^+[Sb_2F_{11}]^- + CF_3OH \quad (3)$$

$$CF_3OH + HF + 2SbF_5 \rightarrow [CF_3OH_2]^+[Sb_2F_{11}]^- \quad (4)$$

Table 1. Crystallographic Data for $[(CH_3)_2OCF_3]^+[Sb_2F_{11}]^-$

chem formula	$C_3H_6F_{14}OSb_2$	ρ_{calcd}, g cm^{-3}	2.820
fw	567.58	Z	4
space group	$Cmc2_1$ (No. 36)	λ, Å	0.710 73
a, Å	9.293(6)	μ, cm^{-1}	0.4199
b, Å	12.456(7)	T, °C	−125
c, Å	11.548(8)	$R_F{}^a$	0.023
V, Å3	1336(1)	$R_w{}^b$	0.063

[a] $R_F = \sum(F_o - F_c)/\sum(F_o)$. [b] $R_w = [\sum[w(F_o{}^2 - F_c{}^2)^2]/\sum(wF_o{}^4)]^{1/2}$.

Table 2. Selected Bond Lengths (Å) and Angles (deg) for $[(CH_3)_2OCF_3]^+[Sb_2F_{11}]^-$

	obsd	calcd
C(1)−O	1.508(8)	1.511
C(2)−O	1.448(9)	1.484
C(2)−F(10)	1.256(14)	1.312
C(2)−F(11)	1.292(9)	1.303
C(3)−H(6)		1.085
C(3)−H(10)		1.082
C(3)−H(11)		1.083
Sb(1)−F(4)	2.033(5)	
Sb(2)−F(4)	2.027(5)	
C(1)−O−C(1a)	112.6(7)	113.7
C(1)−O−C(2)	115.6(4)	114.8
Sb(1)−F(4)−Sb(2)	150.7(4)	

The $[(CH_3)_2OCF_3]^+[Sb_2F_{11}]^-$ salt can be stored at −70 °C for several weeks without decomposition. When thermally decomposed at −40 °C, F_2CO, CH_3F, and SbF_5 are formed (eq 5). The F_2CO and CH_3F products were identified in the gas phase by their IR spectra.

$$[(CH_3)_2OCF_3]^+[Sb_2F_{11}]^- \xrightarrow{-40\ °C} COF_2 + 2CH_3F + 2SbF_5 \quad (5)$$

Crystal Structure of $[(CH_3)_2OCF_3]^+[Sb_2F_{11}]^-$. The crystal data for $[(CH_3)_2OCF_3]^+[Sb_2F_{11}]^-$ are summarized in Table 1. Intensity data (Mo Kα radiation, $\omega-2\theta$ scans, −125 °C) were converted to structure factor amplitudes and their esd's by corrections for background scan speed, crystal decay, and Lorentz and polarization effects. Experimental absorption corrections were applied to the data (ψ scans). The structure was solved by direct methods and refined by standard least-squares and Fourier techniques. The positions of all non-hydrogen atoms were refined with anisotropic thermal parameters. The H atoms were placed at the calculated sites. Selected bond lengths and angles are summarized in Table 2 and are compared to the values calculated at the B3LYP/6-311++G(2d,2p) level for the free gaseous cation.

The cations and anions of $[(CH_3)_2OCF_3]^+[Sb_2F_{11}]^-$ are located on mirror planes and possess the characteristic symmetry C_s. They are weakly associated through O(1)- - -F(1) contacts of 2.998 Å that approximate the sum of their van der Waals radii of 2.99 Å and extend the coordination of the oxygen atom from trigonal pyramidal to distorted tetrahedral (Figures 1 and 2). The displacement ellipsoids indicate a rotational disorder that mainly involves the atoms F(5), F(7), F(8), and F(10), which are located the farthest from the center of gravity of the two

---

(15) Becke, A. D. *J. Chem. Phys.* **1993**, *98*, 5648.
(16) Frisch, M. J.; Pople, J. A.; Binkley, J. S. *J. Chem. Phys.* **1984**, *80*, 3265.
(17) Gauss, J. *Chem. Phys. Lett.* **1992**, *27*, 614.
(18) Ditchfield, R. *Mol. Phys.* **1974**, *27*, 789.
(19) Hegge, J.; Hoge, B.; Christe, K. O. To be submitted for publication.

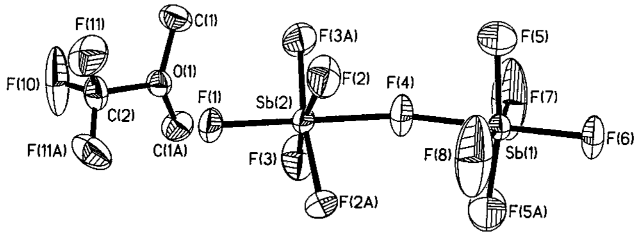

Figure 1. Structure and numbering scheme of $[(CH_3)_2OCF_3]^+[Sb_2F_{11}]^-$. The displacement ellipsoids are drawn at the 50% probability level.

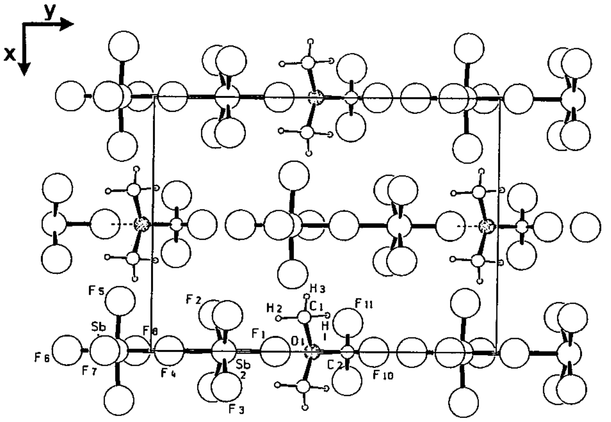

Figure 2. Packing diagram and fluorine bridging in $[(CH_3)_2OCF_3]^+$-$[Sb_2F_{11}]^-$.

ions. Refinements either in the monoclinic space group *Cc* instead of *Cmc*2_1 or as an inversion twin crystal lead to the same structural results.

Since the CF_3 group is larger than a methyl group, the C_H-O-C_F angle of 115.6(4)° in $[(CH_3)_2OCF_3]^+$ is significantly larger and the C_H-O-C_H angle of 112.6(7)° is somewhat smaller than that of 113.1(7)° observed for $[(CH_3)_3O]^+$ in its $[BF_4]^-$ salt.[4] As a result, the sum of the C−O−C bond angles in $[(CH_3)_2OCF_3]^+$ is 4.5° larger than that in $[(CH_3)_3O]^+$. Whereas for the first-row-element species $[(CH_3)_3O]^+$ and $(CH_3)_3N$ the replacement of hydrogens by fluorines significantly increases the repulsion among the methyl groups,[4,6] no pronounced effect was observed for the corresponding phosphorus and arsenic compounds due to decreased steric crowding.[20−23] Obviously the repulsive effects of the fluorine lone pairs are more pronounced when combined with small central atoms such as nitrogen or oxygen.

Fluorine substitution in the trimethyloxonium ion also causes a shortening of the $O-C_F$ and a lengthening of the $O-C_H$ bonds by $\Delta r = 0.03(1)$ Å, relative to the $O-C_H$ bond of 1.477(7) Å in $[O(CH_3)_3]^+$.[4] This change is comparable to that of 0.032(6) Å observed for the N−C bonds in $(CH_3)_3N$ and $(CF_3)_3N$.[6] The increased $O-C_H$ bond length in $[(CH_3)_2OCF_3]^+$ indicates that the latter should be a stronger alkylating agent than $[O(CH_3)_3]^+$. In the strongest previously known methylating agent, the methoxythionyl cation ($[OSOCH_3]^+$),[24] the C−O bond length of 1.49(2) Å is similar to the value of 1.508(6) Å found for $[(CH_3)_2OCF_3]^+[Sb_2F_{11}]^-$. Since $[CH_3OHCF_3]^+$ was shown in our study to readily methylate CH_3OCF_3 to $[(CH_3)_2OCF_3]^+$ (eq 3), the $[CH_3OHCF_3]^+$ cation should be an even stronger methylating agent, although not as powerful as the CH_3F/SbF_5 system itself from which it was formed. Extrapolation of the observed trends suggests that the methylating power of the $[(CH_3)_2OCF_3]^+$ cation should further increase when a second methyl group is replaced by a trifluoromethyl group.

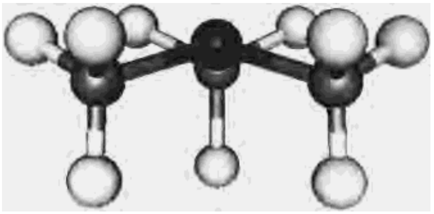

Figure 3. Calculated structure of the free gaseous $[(CH_3)_2OCF_3]^+$-$[Sb_2F_{11}]^-$ cation showing the eclipsed nature of the fluorine and hydrogen ligands.

A comparison of the observed and calculated bond lengths in $[(CH_3)_2OCF_3]^+$ (see Table 2) shows fair agreement. As expected, the density functional calculation slightly overestimates the bond lengths. Again, there is a pronounced difference in the lengths of the C_H-O and C_F-O bonds, and the C_F-O-C_H bond angle is larger than the C_H-O-C_H bond angle, although the calculated differences are somewhat smaller than the observed ones. Although the methyl hydrogen atoms were not directly located by the crystal structure determination, their calculated positions are in good agreement with those predicted by the theoretical calculations for the minimum energy structure of the free gaseous ion (see Figure 3). As can be seen, the fluorine atoms are perfectly eclipsed with the methyl hydrogen atoms, indicating a positive interaction between them.

The geometry observed for the $[Sb_2F_{11}]^-$ anion in $[(CH_3)_2OCF_3]^+[Sb_2F_{11}]^-$ is similar to those observed for this anion in other salts. The two SbF_6 octahedra are linked by a common corner with an Sb(1)−F(4)−Sb(2) angle of 150.7(5)° and are staggered with respect to each other.[25−30]

Nuclear Magnetic Resonance Spectra. The experimentally observed and calculated ^{1}H, ^{13}C, and ^{19}F NMR spectra of $[(CH_3)_2OCF_3]^+$, $[(CH_3)_2OCF(CF_3)_2]^+$, and $[(CH_3)_3O]^+$ and of their parent ethers are summarized in Table 3 and confirm the identity of the new cations. As was previously pointed out,[11] the methylation of an ether results in a pronounced deshielding of the α-methyl protons by about 1 ppm and of the α-methyl carbons by about 15−30 ppm. However, the shielding effect of the additional CH_3^+ group on the perfluorinated α-carbons is small and its direction is hard to predict. Similarly, the fluorine atoms of a perfluorinated α-methyl group are little influenced by the methylation, but the single example of an α-CF group in our study exhibits a significant deshielding of about 16 ppm. A second parameter that permits us to distinguish the parent ether from its methylated oxonium salt is the $^1J_{CF}$ coupling constant of the α-CF_n group. In the ether it has a value of about 250 Hz, whereas in the oxonium salt it ranges from about 280 to 290 Hz.

---

(20) Bartell, L. S.; Brockway, O. L. *J. Chem. Phys.* **1960**, *32*, 592.
(21) Marsden, C. J.; Bartell, L. S. *Inorg. Chem.* **1976**, *15*, 2713.
(22) Springall, H. D.; Brockway, L. O. *J. Am. Chem. Soc.* **1938**, *60*, 996.
(23) Bowen, H. J. *Trans. Faraday Soc.* **1954**, *50*, 463.
(24) Gillespie, R. J.; Riddell, F. G.; Slim, D. R. *J. Am. Chem. Soc.* **1976**, *98*, 8069.
(25) Bernhardt, E.; Bley, B.; Wartchow, R.; Willner, H.; Bill, E.; Kuhn, P.; Sham, I. H. T.; Bodenbinder, M.; Broechler, R.; Aubke, F. *J. Am. Chem. Soc.* **1999**, *121*, 7188.
(26) Willner, H.; Bodenbinder, M.; Broechler, R.; Hwang, G.; Rettig, S. J.; Trotter, J.; von Ahsen, B.; Westphal, V. J.; Thiel, W.; Aubke, F. *J. Am. Chem. Soc.* **2001**, *123*, 588.
(27) Drews, T.; Seppelt, K. *Angew. Chem., Int. Ed. Engl.* **1997**, *36*, 273.
(28) Mootz, D.; Bartmann, K.; *Angew. Chem.* **1988**, *100*, 424.
(29) Burgess, J.; Fraser, C. J. W.; McRae, V. M.; Peacock, R. D.; Russel, D. R.; *J. Inorg. Nucl. Chem., Suppl.* **1976**, 183.
(30) McKee, D.; Adams, C. J.; Zalkin, A.; Bartlett, N. *J. Chem. Soc., Chem. Commun.* **1973**, 26.

Table 3. Observed and Calculated[a] NMR Parameters for the Oxonium Salts $[(CH_3)_2OCF_3]^+$, $[(CH_3)_2OCF(CF_3)_2]^+$, and $[(CH_3)_3O]^+$ and Their Parent Ethers

	chem shift, ppm						coupling constant, Hz		
compd	$\delta(^1H)$	$\delta(^{13}CH_3)$	$\delta(^{13}CF_3)$	$\delta(^{13}CF)$	$\delta(C^{19}F_3)$	$\delta(C^{19}F)$	$^1J(^{13}C^{19}F_3)$	$^1J(^{13}C^{19}F)$	$^3J(^{13}C^{19}F)$
CH_3OCF_3[b]	3.47	53.7 q	123.7 q		−65.6		252.3		4.03
	(3.7)	(56.3)	(132.6)		(−68.3)				
$[(CH_3)_2OCF_3]^+$ [b,c]		80.2 q	120.7 q		−66.9		287.0		2.4
	(4.8)	(81.0)	(132.8)		(−67.9)				
$CH_3OCF(CF_3)_2$b	3.13	52.5 s	119.0 q	102.4 d	−81.0	−146.8	287.9	248.0	
$[(CH_3)_2OCF(CF_3)_2]^+$[b,c]	3.79	83.9	115.8 q,d	106.2 d sept	−76.1	−131.1	291.5	280.5	
CH_3OCH_3[d]	3.24	59.4 s							
	(3.2)	(62.9)							
$[(CH_3)_3O]^+$ [d]	4.58	79.3 s							
	(4.4)	(82.2)							

[a] Calculated values (given in parentheses) at the MP2/6-311++G(2d,p) level using the B3LYP geometries. [b] Values from this study recorded at −30 °C in HF solution. [c] Signals due to $[Sb_2F_{11}]^-$ and $[SbF_6]^-$ were observed in the ^{19}F spectra at −93.1, −124.5, and −141.2 ppm with area ratios of 1:8:2 and at −124.5 ppm, respectively. The HF signal was observed at about −185 ppm. [d] Values from: Olah, G. A.; Doggweiler, H.; Felberg, J. D.; Frohlich, S. *J. Org. Chem.* **1985**, *50*, 4847. Olah, G. A.; DeMember, J. R. *J. Am. Chem. Soc.* **1970**, *92*, 2562.

Table 4. Low-Temperature Raman Spectrum of $[(CH_3)_2OCF_3]^+[Sb_2F_{11}]^-$ and Its Assignments Based on the Frequencies and Intensities Calculated at the B3LYP Level for the Free Gaseous Cation in Point Group C_s

	calcd (B3LYP) free $[(CH_3)_2OCF_3]^+$			obsd $[(CH_3)_2OCF_3]^+[Sb_2F_{11}]^-$
approx mode descripn[a]	freq, cm^{-1}	[Ra int][b]	(IR int)[c]	freq, cm^{-1}
$\nu_1(A')\ \nu_{as}(CH_2)$ in phase	3229	[38.7]	(8.0)	3110[3]
$\nu_{19}(A'')\ \nu_{as}(CH_2)$ out of phase	3227	[21.2]	(3.7)	
$\nu_2(A')\ \nu_{as}(CH_2')$ in phase	3212	[52.2]	(3.9)	3100[2]
$\nu_{20}(A'')\ \nu_{as}(CH_2')$ out of phase	3210	[4.2]	(0.45)	
$\nu_3(A')\ \nu_{sym}(CH_3)$ in phase	3099	[199.6]	(0.44)	3002[9]
$\nu_{21}(A'')\ \nu_{sym}(CH_3)$ out of phase	3096	[0.05]	(0.45)	
combination bands				2859[1]
				2841[0+]
$\nu_4(A')\ \delta_{sym}(CH_3)$ in phase	1498	[0.98]	(58.7)	
$\nu_5(A')\ \delta_{sciss}(CH_2')$ in phase	1491	[4.5]	(19.7)	
$\nu_6(A')\ \delta_{sciss}(CH_2')$ in phase	1484	[2.5]	(0.76)	1444[2]
$\nu_{22}(A'')\ \delta_{sciss}(CH_2)$ out of phase	1479	[7.6]	(0.18)	
$\nu_{23}(A'')\ \delta_{sciss}(CH_2')$ out of phase	1472	[0.17]	(13.3)	
$\nu_{24}(A'')\ \delta_{sym}(CH_3)$ out of phase	1451	[0.42]	(2.6)	
$\nu_{25}(A'')\ \nu_{as}(CF_3)$	1347	[0.75]	(325.9)	
$\nu_7(A')\ \nu_{as}(CF_3)$	1294	[0.81]	(312.0)	
$\nu_8(A')\ \delta_{wag}(CH_3)$ in phase	1253	[0.98]	(30.6)	
$\nu_9(A')\ \delta_{rock}(CH_3)$ in phase	1188	[0.97]	(1.2)	1183[0+]
$\nu_{26}(A'')\ \delta_{wag}(CH_3)$ out of phase	1161	[0.78]	(0.71)	1160[0+]
$\nu_{27}(A'')\ \delta_{rock}(CH_3)$ out of phase	1133	[1.2]	(1.4)	1135[0+]
$\nu_{10}(A')\ \nu_{sym}(CF_3)$	1042	[0.47]	(275.3)	1096[0+]
$\nu_{28}(A'')\ \nu_{as}(OC_2(H))$	899	[1.4]	(85.1)	894[1]
$\nu_{11}(A')\ \nu(O{-}CF_3)$	806	[5.8]	(224.5)	858[2]
$\nu_{12}(A')\ \nu_{sym}(OC_2(H))$	756	[8.6]	(55.7)	759[8]
				676[100]
Sb−F stretching				652[24]
				616[5]
$\nu_{13}(A')\ \delta_{as}(CF_3)$	607	[1.1]	(5.3)	610[2]
$\nu_{29}(A'')\ \delta_{as}(CF_3)$	583	[1.9]	(4.1)	594[2]
$\nu_{14}(A')\ \delta_{sym}(CF_3)$	536	[5.5]	(3.4)	551[4]
$\nu_{15}(A')\ \delta_{rock}(CF_3)$	427	[0.97]	(2.3)	438[0+]
$\nu_{30}(A'')\ \delta_{as}(OCF_2)$	402	[1.4]	(15.8)	415[2]
$\nu_{16}(A')\ \delta_{sym}(C_3O)$	348	[1.1]	(1.1)	367[1]
				306[12]
Sb−F deformations				294[10]
				276[1]
$\nu_{31}(A'')\ \delta_{as}(C_3O)$	274	[0.001]	(0.45)	231[14]
$\nu_{17}(A')\ \delta(C_3O)$ out of phase	215	[0.30]	(5.8)	210[1]
$\nu_{18}(A')\ \tau(CH_3)$ in phase	157	[0.10]	(0.22)	
$\nu_{32}(A'')\ \tau(CH_3)$ out of phase	133	[0.08]	(0.27)	
$\nu_{33}(A'')\ \tau(CF_3)$	56	[0.23]	(0.44)	

[a] Mode description is based on the potential energy distribution. [b] Calculated Raman intensities in Å^4/amu. [c] IR intensities in km/mol.

The observed NMR shifts of these compounds were confirmed by theoretical calculations at the MP2/6-311++G(2d,p) level. As can be seen from Table 3, the agreement between the observed and calculated values is very good and supports the above conclusions concerning the changes one might expect when methylating such ethers.

Vibrational Spectra. Figure 4 shows the low-temperature Raman spectrum of solid $[(CH_3)_2OCF_3]^+[Sb_2F_{11}]^-$. The observed frequencies and their assignments in point group C_s are summarized in Table 4. The assignments were made by a comparison with the frequencies and Raman intensities calculated for the free $[(CH_3)_2OCF_3]^+$ cation at the B3LYP/6-

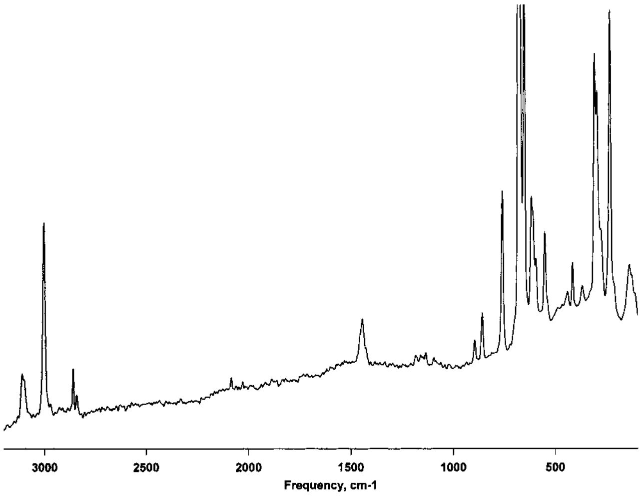

Figure 4. Low-temperature Raman spectrum of $[(CH_3)_2OCF_3]^+[Sb_2F_{11}]^-$.

311++G(2p,2d) level of theory. The agreement between the observed and calculated values is good and the assignments, derived from the calculated potential energy distribution, do not require any further discussion. The remaining bands are due to the $[Sb_2F_{11}]^-$ anion and are in reasonable agreement with those of other $[Sb_2F_{11}]^-$ salts,[25,26,31,32] particularly if the large variation in the structures of $[Sb_2F_{11}]^-$ in its different salts is kept in mind.

Acknowledgment. The work at USC and the Air Force Research Laboratory was supported by the National Science Foundation and the Air Force Office of Scientific Research, respectively. B.H. and J.H. are grateful to the Deutsche Forschungsgemeinschaft for stipends.

Supporting Information Available: Crystal data and structure refinement parameters (Table S1), atomic coordinates and equivalent isotropic displacement parameters (Table S2), all bond lengths and angles (Table S3), anisotropic thermal parameters (Table S4), and hydrogen coordinates and isotropic displacement parameters (Table 5) as well as crystallographic data files in CIF format. This material is available free of charge via the Internet at http://pubs.acs.org.

IC010239W

---

(31) Christe, K. O.; Schack, C. J.; Wilson, R. D. *Inorg. Chem.* **1976**, *15*, 1275.

(32) Vij, A.; Wilson, W. W.; Vij, V.; Tham, F. S.; Sheehy, J. A.; Christe, K. O. *J. Am. Chem. Soc.*, in press.